Published in final edited form as:
Free Radic Biol Med. 2010 November 1; 49(8): 1255–1262. doi:10.1016/j.freeradbiomed.2010.07.006.

Loss of manganese superoxide dismutase leads to abnormal growth and signal transduction in mouse embryonic fibroblasts

Yiqiang Zhang[1,4,5], **Hong-Mei Zhang**[3], **Yun Shi**[1], **Michael Lustgarten**[1], **Yan Li**[4], **Wenbo Qi**[4], **Bin-Xian Zhang**[3], and **Holly Van Remmen**[1,2,4,5]

[1]Department of Physiology, University of Texas Health Science Center at San Antonio, San Antonio, Texas 78229

[2]Department of Cellular and Structural Biology, University of Texas Health Science Center at San Antonio, San Antonio, Texas 78229

[3]Department of Medicine, University of Texas Health Science Center at San Antonio, San Antonio, Texas 78229

[4]Barshop Institute for Longevity and Aging Studies, University of Texas Health Science Center at San Antonio, San Antonio, Texas 78229

[5]South Texas Veterans Health Care System, San Antonio, Texas 78229

Abstract

Manganese superoxide dismutase (MnSOD) in the mitochondria plays an important role in cellular defense against oxidative damage. Homozygous MnSOD knockout (*Sod2*$^{-/-}$) mice are neonatal lethal, indicating the essential role of MnSOD in early development. To investigate the potential cellular abnormalities underlying the aborted development of *Sod2*$^{-/-}$ mice, we examined the growth of isolated mouse embryonic fibroblasts (MEF) from *Sod2*$^{-/-}$ mice. We found that the proliferation of *Sod2*$^{-/-}$ MEFs was significantly decreased when compared with wild type MEFs despite the absence of morphological differences. The *Sod2*$^{-/-}$ MEFs produced less cellular ATP, had lower O_2 consumption, generated more superoxide, and expressed less Prdx3 protein. Furthermore, the loss of MnSOD dramatically altered several markers involved in cell proliferation and growth, including decreased growth stimulatory function of mTOR signaling and enhanced growth inhibitory function of GSK-3β signaling. Interestingly, the G protein coupled receptor-mediated intracellular Ca^{2+} ($[Ca^{2+}]_i$) signal transduction was also severely suppressed in *Sod2*$^{-/-}$ MEFs. Finally, the ratio of LC3-II/LC3-I, an index of autophagic activity, was increased in *Sod2*$^{-/-}$ MEFs, consistent with a reduction of mTOR signal transduction. These data demonstrate that MnSOD deficiency results in alterations in several key signaling pathways, which may contribute to the lethal phenotype of *Sod2*$^{-/-}$ mice.

Keywords

MnSOD; oxidative stress; ROS; signal transduction

To whom correspondence should be addressed: Holly Van Remmen, Ph.D., Department of Cellular and Structural Biology, Barshop Institute for Longevity and Aging Studies, University of Texas Health Science Center at San Antonio, 15355 Lambda Drive, San Antonio, Texas 78245, Tel: (210) 562-6141, Fax: (210) 562-6110, vanremmen@uthscsa.edu.

Introduction

Oxidative stress plays an important role in the pathogenesis and/or progression of a variety of diseases including neurodegenerative diseases, ischemia-reperfusion injury in the brain and heart, diabetes, and other aging-related diseases [1–4]. Superoxide and other reactive oxygen species (ROS) in cells are mainly produced during substrate oxidation by complex I and complex III of the mitochondrial electron transport chain [5]. Under normal conditions, superoxide anion is rapidly dismutated by MnSOD, a nuclear encoded (*Sod2*) and mitochondrial matrix-localized antioxidant enzyme that converts superoxide into hydrogen peroxide. Superoxide that escapes removal by MnSOD can react with nitric oxide to form peroxynitrite and leads to further oxidative modification of cellular components. Thus, removal of superoxide by MnSOD is a critical component of cellular antioxidant protection.

Attempts to create mouse models with homozygous deletion of the *Sod2*$^{-/-}$ gene have not been successful because *Sod2* deletion leads to a lethal phenotype [6–8]. Although the phenotypic manifestations of *Sod2* knockout mice vary with different genetic backgrounds, no viable siblings survive beyond a few weeks after birth. In contrast, *Sod2*$^{+/-}$ mice are viable and do not have a shortened life span [9]. However, *Sod2*$^{+/-}$ mice show increased sensitivity to apoptosis, increased oxidative damage, and impaired mitochondrial respiration in various tissues [9–13]. The lethality of *Sod2* null mice may result from severe damage caused by excessive superoxide [10, 11, 14–17]. Indeed, mouse embryonic fibroblasts (MEF) from *Sod2*$^{-/-}$ mice have elevated cellular superoxide and an abnormal cell cycle when compared with wild-type MEFs [18].

The mammalian target of rapamycin (mTOR)-dependent signaling pathway plays a central regulatory role in cell growth and metabolism in response to nutrients, growth factors, cellular energy, and stress [19–21]. Therefore, it is possible that increased oxidative stress from *Sod2* deletion may lead to abnormal mTOR-dependent signaling, thus contribute to the early death of *Sod2*$^{-/-}$ mice. It has also been shown that amino acid response of mTOR complex 1 (mTORC1) is dependent on intracellular Ca^{2+} mobilization ($[Ca^{2+}]_i$) and superoxide generation [22, 23]. Furthermore, α_{1A}-adrenergic receptor (G protein coupled receptor) has been shown to activate mTOR signaling via $[Ca^{2+}]_i$ mobilization and phosphatidic acid [24]. Therefore, we speculate that changes of superoxide levels in *Sod2*$^{-/-}$ mice might also affect Ca^{2+} mobilization and its related signaling pathways.

In this study, we examined MEFs cultured from wild-type control and *Sod2*$^{-/-}$ mouse embryos to investigate the possible mechanism(s) that might contribute to the early death of *Sod2*$^{-/-}$ mice. We found that the proliferation rate of *Sod2*$^{-/-}$ MEFs decreased significantly when compared to wild-type MEFs and that *Sod2*$^{-/-}$ MEFs had reduced cellular ATP levels, impaired O_2 consumption, reduced expression of Prdx3, and enhanced superoxide generation. Furthermore, we found alterations in the mTOR signaling pathways and the G protein coupled receptor-mediated intracellular Ca^{2+} ($[Ca^{2+}]_i$) signal transduction in *Sod2*$^{-/-}$ cells, which are consistent with reduced proliferation and increased autophagy, suggesting a role for O_2^- in these signaling pathways.

Materials and Methods

Chemicals and Antibodies

Hydrogen peroxide, rapamycin, antimycin A, rotenone, bradykinin, and carbonyl cyanide *p*-(tri-fluromethoxy) phenyl-hydrazone (FCCP) were purchased from Sigma-Aldrich (St. Louis, MO). The MnSOD mimetic, MnTBAP was purchased from Oxis International (Beverly Hills, CA). Antibodies against 4EBP1, S6K1, GSK-3β, S6, Akt and their respective phosphorylated forms were purchased from Cell Signaling (Danvers, MA).

Antibody against LC3 was purchased from Novus (Littleton, CO). Antibodies against MnSOD, CuZnSOD were purchased from Assay Design (Ann Arbor, MI). Antibody against Gpx4, Gpx1, Prdx3, Prdx1, Trx1, and Trx2 were purchased from Abcam (Cambridge, MA). Antibodies against mitochondrial complex I 20 kDa subunit and complex III core I subunit were purchased from Invitrogen (Carlsbad, CA). Dihydroethidium (DHE) and fura-2 AM was purchased from Invitrogen (Carlsbad, CA).

Cell culture

Mouse embryonic fibroblasts (MEFs) were isolated from pregnant mice at day 12 to day 14 post coitus following standard protocols as described previously [25]. We compared 3 individual lines of *Sod2*$^{-/-}$ and wild type MEFs which were maintained in complete Dulbecco's modified eagles medium (DMEM) supplemented with 10% fetal bovine serum at 37°C in a humidified incubator with 5% CO_2. Without further indication, all experiments were conducted using MEFs within five passages post isolation. Without specification in the text or figure legends, the data were representative of one pair of the wild type and *Sod2*$^{-/-}$ MEFs.

The cell proliferation assay was carried out in 24-well tissue culture plates at an initial plating density of 5×10^3 cells per well. Cell number or viability was monitored using the MTT assay (Sigma, St. Louis, MO) following the manufacturer's instructions and cell enumeration using haemocytometer. Day zero was designated as the day of initial plating of the cells. Treatment of cells with different reagents was also conducted at day zero (concentrations used are described in the text and figure legends).

Western blot analysis

Cells were disrupted in RIPA buffer (1x PBS, 1% Nonidet P-40, 0.5% sodium deoxycholate, 0.1% SDS) on ice supplemented with inhibitors of protease and phosphatase (Roche, Indianapolis, IN). The supernatant was collected after centrifugation at 4 °C, 12000 × g for 10 minutes. Proteins were separated on SDS-PAGE gel followed by transferring to nitrocellulose membrane. Target proteins were detected with the following specific monoclonal or polyclonal antibodies: actin, HPRT, Gpx4, Gpx1, SOD2, SOD1, Prdx3, Prdx1, Trx1, Trx2, catalase, mitochondrial complex I 20 kD subunit, complex III 50 kD core; 4EBP1, phospho-4EBP1 (Thr37/46), p76SK, phospho-p76SK (Thr389), GSK-3β, phospho-GSK-3β (Ser9), Akt, phospho-Akt (Ser473), S6, phospho-S6 (Ser235/236), and LC3. To compare the band intensity between two groups of cells, the total or phosphorylated proteins were first each normalized to house keeping gene, β-actin, and then compared to each other.

Cell metabolism and mitochondrial function

ATP generation in MEFs was analyzed by the luciferase substrate assay (Invitrogen, Carlsbad, CA). Briefly, $1 – 2 \times 10^6$ cells were washed once with HBSS and suspended in 400 μl of TE buffer (100 mM Tris-Cl, pH7.5, 4 mM EDTA). The samples were boiled for 3 minutes and chilled on ice. The supernatant, after centrifugation at 12000 × g for 5 minutes, was used for ATP measurement in a 96-well plate.

Oxygen consumption (OCR) was measured using both the extracellular flux analyzer (Seahorse Bioscience XF24) and the Oxytherm oxygen electrode detection system (Hansatech, Norfolk, England) following the manufacturers' instructions. Briefly, when using the extracellular flux analyzer, MEFs were plated one day before analysis at a density of 1×10^4 cells per well. The sensor plate was incubated the same day with 750 ml calibration buffer at 37°C without CO_2 for 24 hours. On the day of analysis, the culture medium was replaced with 700 μL respiration medium and incubated at 37 °C without CO_2

for at least 2 hours. Before calibration, 75 μL of 25 μM FCCP was aliquoted into each chamber in the sensor plate (after sequential injection, the final concentration of FCCP is approximately 2.5, 5, 7.5, and 10 μM). Addition of FCCP uncouples the respiratory chain from ATP synthesis, thereby removing negative feedback and allowing the respiratory chain to work at a maximal rate. Oxygen consumption was measured before FCCP injection and after sequential injection of FCCP. To analyze O_2 consumption using the Oxytherm system, the cells were harvested from near confluent culture dishes and resuspended in ROS buffer after washed with 1x PBS. One million cells in 20 μl volume were aliquoted into the equilibrated pre-assembled electrode chamber. The rate of O_2 consumption was first measured after adding ADP to a final concentration of 4 mM, and then measured after adding FCCP (10 μM final) to completely uncouple the oxidative phosphorylation processes.

Measurement of $[Ca^{2+}]_i$ in MEF cells

MEFs grown in 100 mm dishes were labeled with fura-2 (1 μM) at 37°C for 30 minutes in RPMI 1640 medium to measure $[Ca^{2+}]_i$. Loaded cells were harvested and resuspended in PBS1Ca buffer (containing 1 mM KH_2PO_4, 3 mM Na_2HPO_4, 154 mM NaCl, 1 mM $CaCl_2$, 1 mM $MgSO_4$, pH 7.4). $[Ca^{2+}]_i$ mobilization was monitored in a fluorometer (QM-6, Photon Technology International, Birmingham, NJ) using a cuvette with the temperature stabilized at room temperature. The ratio of fluorescence excited at 340 and 380 nm with emission of 510 nm was recorded and used to index the $[Ca^{2+}]_i$ change as previously reported [26].

Transcription quantification by RT-PCR

RNA was isolated from MEFs using TRI reagent (Invitrogen) following the manufacturer's instructions. An equal amount of RNA was reversely transcribed into cDNA using a RETROscript kit (Ambion, Austin, TX) according to the manufacturer's protocol. The reverse transcribed cDNA was subjected to polymerase chain reaction using the GeneAmp 7700 sequence detection system (Applied Biosystem, Foster City, CA). The reactions were performed with 40 cycles (15 seconds at 95°C; 1 minute at 62°C). Each sample was measured in triplicate. Quantification was performed according to the manufacturer's suggestions. Actin was used as the reference gene for normalization.

Analysis of ROS content

ROS (superoxide) generation was detected by cytofluorimetric analysis using the fluorescent probe DHE (excitation at 544 nm and emission at 612 nm) at 37°C. Equal numbers of wild-type and MnSOD-null cells were incubated with 50 μM of DHE for 30 minutes at 37°C in the dark. After incubation, cells were washed once with 1X PBS, and resuspended in 1X PBS. 1×10^5 cells from each sample were aliquoted into one well of a 96-well plate for fluorescence intensity analysis on a FACSCalibur instrument. Cells without DHE were used as background control.

Analysis of oxidative damage

Oxidative damage of macromolecules in the cell, specifically lipid oxidation was analyzed as previously described [27]. Briefly, $3–4 \times 10^6$ cells were harvested and washed once with 1X PBS buffer. Lipid oxidation was assessed by measuring the content of F_2-isoprostanes, following the procedure exactly as described by Roberts et al [28], which involves lipid extraction with chloroform, thin layer chromatography (TLC) purification, and quantification by gas chromatography–mass spectrometric analysis.

Statistical analysis

The results are presented as means ± SEM. Statistical evaluation was conducted by ANOVA one-way or two-way analysis, followed by the *post hoc* Bonferroni test. Differences were considered significant at $p < 0.05$.

Results

Elevated cellular superoxide and oxidative injury in Sod2$^{-/-}$ MEF

Mitochondrial superoxide is converted to hydrogen peroxide by MnSOD located in the mitochondrial matrix. It is expected that in the absence of MnSOD, the conversion of superoxide to hydrogen peroxide would be severely impaired in *Sod2*$^{-/-}$ MEFs. As shown in Figure 1A, *Sod2*$^{-/-}$ MEFs have significantly higher levels of superoxide than wild type control cells (as indexed by an enhanced DHE fluorescent intensity, which measures superoxide preferentially [29]). The elevated superoxide in *Sod2*$^{-/-}$ MEFs was also confirmed by EPR (Electron Paramagnetic Resonance) method (data not shown). The increased superoxide present in *Sod2*$^{-/-}$ MEFs is associated with significantly enhanced oxidative damage to lipids as indicated by a higher concentration of isoprostanes (Figure 1B).

The lack of MnSOD in *Sod2*$^{-/-}$ MEFs would impair the proper removal of superoxide in the cells and the resultant oxidative damage may lead to increased sensitivity to superoxide inducers. Inhibition of mitochondrial complex I or complex III stimulates superoxide production in various cell types and as a result, the lack of MnSOD may render the cells prone to oxidative damage. As shown in Figure 1C, treatments with rotenone (a respiratory chain complex I inhibitor) or antimycin A (a respiratory chain complex III inhibitor) caused significantly more cell death in MEFs isolated from *Sod2*$^{-/-}$ than those from wild-type control mice ($p < 0.05$, control vs. *Sod2*$^{-/-}$), indicating that *Sod2*$^{-/-}$ MEFs are more susceptible to the oxidative damage induced by increased superoxide generation in response to rotenone and antimycin A.

Expression of anti-oxidative stress proteins in Sod2$^{-/-}$ MEFs

MnSOD deletion and enhanced superoxide levels in *Sod2*$^{-/-}$ MEFs may be compensated for by alterations of other anti-oxidative stress mechanisms [11, 30]. We thus examined the expression of several known anti-oxidative stress enzymes including catalase, glutathione peroxidase1 and 4 (Gpx1, 4), peroxiredoxin 1 and 3 (Prdx1, 3), thioredoxin 1 and 2 (Trx1, 2), and superoxide dismutase 1 (SOD1) in *Sod2*$^{-/-}$ MEFs. As indicated in Figure 2, no significant changes of protein expression in catalase, Gpx1, Gpx4, Trx1, Trx2, Prdx1 and SOD1 in *Sod2*$^{-/-}$ MEFs when compared with wild-type controls. However, the expression of Prdx3, an important enzyme in the mitochondria that detoxifies hydrogen peroxide, was dramatically reduced (>70% reduction). The expression of Prdx3 was not due to reduced transcription because no changes of mRNA were detected in *Sod2*$^{-/-}$ MEFs. Furthermore, no significant changes were detected in subunits of two mitochondrial respiratory complexes, complex I and III.

Reduced proliferation and impaired mitochondrial function in Sod2$^{-/-}$ MEFs

Superoxide-induced damage may alter cell proliferation and contribute to the neonatal death of *Sod2*$^{-/-}$ mice. To detect abnormal cell proliferation, equal numbers of control and *Sod2*$^{-/-}$ MEFs were cultured under same conditions, and the changes in cell number were continuously monitored for a 5-day period. As shown in Figure 3A, the cell number of *Sod2*$^{-/-}$ MEFs at all subsequent time points was significantly less than control, indicating a reduced proliferation rate.

The reduced proliferation of the *Sod2*$^{-/-}$ MEFs was found to be associated with altered oxygen consumption and ATP production. As shown in Figure 3B, the cellular ATP level in *Sod2*$^{-/-}$ MEFs was found to be significantly lower when compared with the wild-type cells, suggesting increased energy consumption or impaired ATP generation in *Sod2*$^{-/-}$ cells. As shown in Figure 3C, the basal level of oxygen consumption was similar between wild-type and *Sod2*$^{-/-}$ MEFs. However, the maximal rate of oxygen consumption (induced by FCCP) was significantly lower in *Sod2*$^{-/-}$ MEFs, indicating a defective respiratory chain in *Sod2*$^{-/-}$ cells.

Impaired intracellular Ca^{2+} signaling in Sod2$^{-/-}$ MEFs

Studies have demonstrated that excessive production of ROS could change redox signaling and calcium handling inside the cell [31]. Therefore, deletion of superoxide dismutase, which leads to the increase of ROS, could affect calcium flux and signaling. It has been previously shown that *Sod1* mutant SOD1(G93A) perturbs Ca^{2+} homeostasis and is associated with amyotrophic lateral sclerosis in mice [32]. Whether MnSOD deficiency (*Sod2*$^{-/-}$) affects Ca^{2+} homeostasis is currently unknown. In the experiments shown in Figure 4, we have examined the impact of *Sod2* deletion on intracellular Ca^{2+} ($[Ca^{2+}]_i$) signaling responsive to G-protein coupled receptor agonists (bradykinin and ATP) and fatty acids using *Sod2*$^{-/-}$ MEFs. The amplitudes of the $[Ca^{2+}]_i$ responses of bradykinin (BK, 100nM), ATP (100μM), and linoleic acid (30 μM) were significantly reduced in *Sod2*$^{-/-}$MEFs, when compared with controls (Figure 4A–C). However, unlike the $[Ca^{2+}]_i$ responses induced by the G-protein coupled receptor agonists BK and ATP, linoleic acid was shown to induce $[Ca^{2+}]_i$ mobilization in a different manner [26, 33, 34], suggesting that MnSOD deficiency has a profound effect on Ca^{2+} homeostasis.

Abnormal mTOR signaling in Sod2$^{-/-}$ MEF

The mTOR signaling pathway serves as a central regulator for cell growth and stress response. Aberrant mitochondrial function and disturbance of ROS generation may affect multiple cellular signaling pathways and cell growth [35]. Furthermore, aberrant Ca^{2+} homeostasis could also affect mTOR signaling because Ca^{2+} mediates the mTORC1 response to amino acids [23]. We analyzed the mTOR signaling pathway in *Sod2*$^{-/-}$ MEFs by examining the phosphorylation of proteins up- and down-stream of mTOR. Akt, which is activated following phosphorylation, is an upstream regulator responsible for the activation of mTOR and, the inactivation of glycogen synthase kinase-3 (GSK3) signaling by insulin and insulin-like growth factor-1 [36]. We first detected significantly reduced phosphorylation of Akt (Ser473) in *Sod2*$^{-/-}$ MEFs despite a similar level of total Akt protein found in wild-type cells (Figure 5A). Reduced Akt phosphorylation/activation may be responsible for the decreased mTOR signaling, as indicated by down-regulation of the phosphorylation of mTOR downstream target proteins including 4EBP1 (Thr37/46), p76SK1 (Thr389), and S6 (Ser235/236) (Figure 5B).

Interestingly, in parallel to the decreased mTOR signaling found in *Sod2*$^{-/-}$ MEFs, phosphorylation of GSK3β (Ser9), another downstream target of Akt, was also reduced in *Sod2*$^{-/-}$ MEFs (Figure 5C). A reduction in both mTOR signaling and GSK3β phosphorylation could be partially responsible for the slow proliferation observed in *Sod2*$^{-/-}$ MEFs (Figure 3A).

It is noteworthy that in MEFs isolated from *Sod2*$^{-/-}$, 4EBP1 mRNA and total protein levels were significantly increased by 30% over control MEFs (Figure 5D). No significant difference in total protein was observed for other proteins including p76SK1, S6, and GSK3β when comparing *Sod2*$^{-/-}$ MEFs and wild-type control cells.

In addition to the targets described above, reduced mTOR signaling may also impact autophagic flux in *Sod2*$^{-/-}$ MEFs. Currently, the widely accepted approach to measure autophagic activity in cells is to monitor microtubule-associated protein light chain 3 (LC3), i.e., the conversion of LC3-I to LC3-II or ratio of LC3-II/LC3-I [37]. As shown in Figure 5E, the LC3-II/LC3-I ratio was significantly increased in *Sod2*$^{-/-}$ MEFs, indicating enhanced autophagy activity. The increase in autophagic activity may reinforce the inhibitory action of reduced mTOR signaling on cell proliferation and may contribute to early death of *Sod2*$^{-/-}$ mice.

MnSOD mimetic does not improve the proliferation of Sod2$^{-/-}$ MEF

MnTBAP, a chemical that mimics MnSOD function in converting superoxide to hydrogen peroxide, has been shown to protect cells and animals from oxidative damage [38–41]. We therefore tested whether MnTBAP could reverse the abnormalities found in signal transduction and proliferation of *Sod2*$^{-/-}$ MEFs. As shown in Figure 6A, phosphorylated 4EBP1 levels were lower in *Sod2*$^{-/-}$ MEFs than wild-type controls as shown earlier. Rapamycin at 200 nM inhibited the phosphorylation of 4EBP1 in control and *Sod2*$^{-/-}$ MEFs to a similar degree. Interestingly, treatment of *Sod2*$^{-/-}$ MEFs with MnTBAP (400 μM) for 4 hours restored the phosphorylated 4EBP1 to equivalent or even higher levels as observed in control *Sod2*$^{-/-}$ MEFs, without affecting the total 4EBP1 proteins (Figure 6A). In parallel, the same treatment with MnTBAP also increased the phosphorylated p76SK1 and S6 content found in MEFs isolated from *Sod2*$^{-/-}$ (*data not shown*). In contrast, MnTBAP at similar concentrations did not alter the phosphorylation of 4EBP1 significantly in wild type cells, indicating a different signaling response from *Sod2*$^{-/-}$ MEFs.

Next, we tested whether partial restoration of the abnormal mTOR signaling pathway by MnTBAP in *Sod2*$^{-/-}$ MEFs may improve proliferation. As shown in Figure 6B, MnTBAP at 400 μM failed to increase the proliferation of *Sod2*$^{-/-}$ MEFs to the level of wild-type control MEFs after 5 days of incubation (Figure 6B).

Discussion

MnSOD is one of the primary antioxidant enzymes found in mitochondria and has been targeted for studying the role of oxidative stress in aging. Homozygous deletion of *Sod2* is neonatal lethal in mice, while heterozygous *Sod2* mice developed normally and are not short-lived [6–8, 14]. However, *Sod2*$^{+/-}$ mice have increased oxidative stress and oxidative damage in various tissues, have alterations of mitochondrial function and apoptosis, and have a higher incidence of tumorigenesis [9–12, 42]. The dramatic impact of the *Sod2* homozygous deletion on mouse development demonstrates the importance of the anti-oxidant defense system for animal development and survival. However, its role in aging is not clear [43–45]. Excessive cellular reactive oxygen species have been shown to oxidize macromolecules (DNA, protein, and lipids), to alter redox balance, to alter cell growth and differentiation, and to accelerate the induction of cell death or necrosis [46]. Although, *Sod2*$^{-/-}$ mice have a lethal phenotype, *Sod2*$^{-/-}$ cells have been isolated and are viable [12, 14]. *Sod2*$^{-/-}$ MEFs were previously demonstrated to have delayed proliferation with an abnormal regulation of the cell cycle, although prolonged incubation seems to increase the proliferation rate which may be due to transformation as we observed similar phenomenon [18].

In the present study, we demonstrated that MEFs isolated from *Sod2*$^{-/-}$ mice exhibit (1) increased susceptibility to oxidative stress as induced by rotenone and antimycin A; (2) significant reduction in the level of Prdx3 protein; (3) different patterns of ROS generation; (4) increased lipid oxidation; (5) reduced ATP production and oxygen consumption; and (6) reduced proliferation. The significant reduction of Prdx3 expression is the first to be

reported in *Sod2*$^{-/-}$ cells. Studies have demonstrated that Prdx3 can be oxidatively inactivated, thus leading to accelerated degradation [47]. Prdx3 can also be transcriptionally regulated by the FoxO3a transcriptional factor which can be activated by oxidative stress [48]. Another mechanism may involve the translational suppression due to the decrease of mTOR signaling as observed in this study. However, we did not detect significant changes of Prdx3 transcription in *Sod2*$^{-/-}$ MEFs, suggesting the reduction of Prdx3 protein is not due to transcriptional regulation. Therefore, the reduction of Prdx3 protein in *Sod2*$^{-/-}$ MEFs is likely due to posttranscriptional regulation. Further investigation is required to uncover the mechanism of how Prdx3 protein expression is regulated in *Sod2*$^{-/-}$ MEFs.

The significant differences between *Sod2*$^{+/-}$ and *Sod2*$^{-/-}$ cells may partially explain the reason why *Sod2*$^{+/-}$ mice develop normally, *Sod2*$^{-/-}$ mice do not. The increase of superoxide in *Sod2*$^{-/-}$ MEFs is also consistent with Morten's data obtained from cardiomyocytes isolated from *Sod2*$^{-/-}$ mice [38]. The finding of slower proliferation of *Sod2*$^{-/-}$ cells is also consistent with recently published data using chicken cells depleted of MnSOD [49]. However, other studies demonstrated that overexpression of MnSOD delayed cell cycle in hepatocytes and enhanced G2 phase accumulation in oral squamous carcinoma cells [50, 51]. These seemingly contradictory findings that both deletion of and overexpression of MnSOD reduces cell proliferation suggest a fine tuning of the redox balance in mitochondria. Either more or less MnSOD expression likely tips the balance of the redox status inside the cell, and consequently affects cell cycle and proliferation.

We propose that the *Sod2*$^{-/-}$ cells may provide an excellent model to investigate the mechanism by which endogenous ROS affects cell signaling pathways. Figure 7 represents a simplified diagram of the signaling pathways that could interact with each other and are affected in *Sod2*$^{-/-}$ MEFs. In the present study, we demonstrated that the loss of *Sod2* indeed alters several growth signaling pathways, including the mTOR and GSK-3β signaling. *Sod2*$^{-/-}$ cells have reduced levels of phosphorylation of mTOR downstream proteins including 4EBP1, S6K1, and S6. In addition, the level of total 4EBP1 protein was found to be significantly increased in *Sod2*$^{-/-}$ cells. However, no significant changes in protein expression were observed for S6K1, S6, and Akt. The combination of hypo-phosphorylation and an increased expression of 4EBP1 (which is an inhibitory factor for protein translation) may greatly reduce cell proliferation. On the contrary, the growth inhibitory signaling pathway of GSK-3β was enhanced in *Sod2*$^{-/-}$ cells, as indicated by the hypo-phosphorylation of GSK-3β at Ser9, the inhibitory site targeted by several protein kinases including Akt, p76SK, and p90Rsk. GSK-3 is active in quiescent cells and kept inactive in proliferative cells [52]. Thus, the hypo-phosphorylation of GSK-3 may contribute to the maintenance of *Sod2*$^{-/-}$ cells in a quiescent stage as demonstrated by Sarsour et al. [18]. Therefore, the combination of decreased mTOR signaling and increased GSK-3β activity could contribute to the reduced proliferation found in *Sod2*$^{-/-}$ cells. Furthermore, *Sod2*$^{-/-}$ cells show an increased basal level of autophagic activity, as indicated by a higher ratio of LC3B-II/LC3B-I, possibly a result of the reduction in mTOR signaling and the increase in oxidative stress, both of which have been demonstrated to induce autophagy [53, 54]. The increase in autophagy may not be beneficial to the cells, as has been demonstrated and may even contribute to cell death [55].

Furthermore, we demonstrated that *Sod2*$^{-/-}$ cells exhibit a significant reduction in calcium mobilization. Using bradykinin, the G-coupled protein kinase inhibitor that requires calcium mobilization, we found that calcium mobilization in the *Sod2*$^{-/-}$ cells was significantly reduced compared to the wild-type control cells. This reduction in calcium mobilization may have multiple implications. First, it may inhibit the response of mTOR signaling to amino acids, which requires participation of calcium [23, 24]. Secondly, it also may inhibit many other signaling pathways that require calcium [56, 57]. It has been proposed that

mitochondrial ROS generation and calcium mobilization/signaling interact with each other [31, 58, 59]. Therefore, the deletion of MnSOD, the major mitochondrial superoxide detoxification enzyme, will likely impact calcium mobilization from mitochondria, and may further affect calcium-related signaling in the cytosol.

We also tested the ability of the SOD mimetic, MnTBAP to rescue the slow growth of *Sod2*$^{-/-}$ cells. Addition of MnTBAP partially restored the phosphorylation of 4EBP1. However, its presence failed to restore the growth or the survival of *Sod2*$^{-/-}$ MEFs to the level comparable to wild-type MEFs. This may indicate that the molecular changes in *Sod2*$^{-/-}$ cells are so profound that their growth can not be rescued by just simply restoring anti-oxidative stress capacity. Furthermore, our study does not exclude the possibility that MnTBAP may not reach the mitochondria where most of the oxidative damage is possibly localized due to the loss of MnSOD in mitochondria. However, since MnTBAP is membrane permeable and the incubation time in the present study is long enough, it is unlikely that MnTBAP did not reach mitochondria. Furthermore, the MnTBAP demonstrated an effect on reduction of ROS level in our experiment (data not shown). Therefore, the efficacy of MnTBAP is not a question in our experimental system. The difference between our data and the *in vivo* data reported by Melov et al may reflect the difference between isolated cell system and the whole organism [39]. The discrepancy between the survival of whole organism and individual cell in culture has also been demonstrated in another animal model of which *Sod1*$^{-/-}$ fibroblasts have been difficult to cultivate under variety of conditions but the *Sod1*$^{-/-}$ mice developed normally and can survive up to 20 months of age [14]. Nonetheless, the *Sod2*$^{-/-}$ cells could serve as a useful *in vitro* model to screen antioxidants or other pharmaceutical reagents.

Our study demonstrates that perturbation of intracellular ROS generation could have a profound effect on cell growth, including the inhibition of the mTOR signaling pathway and the activation of the GSK-3β signaling in *Sod2*$^{-/-}$ cells. However, this study does not exclude the participation of other growth signaling pathways, due to the complexity of the effect of ROS on cell signaling [60, 61]. Several questions remain to be addressed. The mechanism by which ROS or oxidative stress affects mTOR signaling is not clearly understood. Whether ROS directly regulates mTOR signaling or via other mediators needs further investigation. Previous studies demonstrate that ROS may affect cell signaling through transcriptional regulation via transcription factors including NFκB and HIF (hypoxia inducing factor) [62]. In our study, the increase of 4EBP1 protein expression in *Sod2*$^{-/-}$ cells may be a result of such transcriptional activity. However, the possibility of post-transcriptional regulation including inhibition of protein degradation can not be excluded. A recent study demonstrated FoxO1 regulated degradation of mTOR components including mTOR, raptor, TSC2, and p76SK, indicating another level of post-transcriptional regulation of the activity of mTOR signaling [63]. Finally, ROS can also directly modulate the enzymatic activities of protein kinases and phosphatases via oxidation-reduction of certain amino acids [62, 64, 65]. Therefore, it is possible that the activity of different enzymes found in the mTOR pathway also may be directly modulated by ROS.

In the present study, we also examined growth signaling pathways from different tissues between *Sod2*$^{+/-}$ and wild type control mice and did not observe any significant differences (*data not shown*), suggesting that the level of MnSOD expression is critical for the changes of growth signaling and that MnSOD expression may play an important role in determining the outcome of animal development. Therefore, the dramatic alteration of growth signaling in *Sod2*$^{-/-}$ cells could provide an explanation of why *Sod2*$^{-/-}$ mice could not develop normally and survive.

In conclusion, our study demonstrates a likely association between mitochondrial redox regulation and growth signaling. Perturbation of the mitochondrial ROS balance may have profound effect on cellular signaling and thus on whole animal development.

Acknowledgments

The authors thank Corinne Price for helping editing this manuscript. This study was supported by a Department of Veterans Affairs Merit Grant to HVR.

Abbreviations

MnSOD	magnesium superoxide dismutase
ROS	reactive oxygen species
mTOR	mammalian target of rapamycin
MEF	mouse embryonic fibroblast
Prdx3	peroxiredoxin 3

References

1. Knight JA. Free radicals: their history and current status in aging and disease. Ann Clin Lab Sci. 1998; 28(6):331–346. [PubMed: 9846200]
2. McCord JM. Superoxide dismutase in aging and disease: an overview. Methods Enzymol. 2002; 349:331–341. [PubMed: 11912924]
3. Lenzen S. Oxidative stress: the vulnerable beta-cell. Biochem Soc Trans. 2008; 36(Pt 3):343–347. [PubMed: 18481954]
4. Bashan N, Kovsan J, Kachko I, Ovadia H, Rudich A. Positive and negative regulation of insulin signaling by reactive oxygen and nitrogen species. Physiol Rev. 2009; 89(1):27–71. [PubMed: 19126754]
5. Henderson JR, Swalwell H, Boulton S, Manning P, McNeil CJ, Birch-Machin MA. Direct, real-time monitoring of superoxide generation in isolated mitochondria. Free Radic Res. 2009; 43(9):796–802. [PubMed: 19562601]
6. Li Y, et al. Dilated cardiomyopathy and neonatal lethality in mutant mice lacking manganese superoxide dismutase. Nat Genet. 1995; 11(4):376–381. [PubMed: 7493016]
7. Lebovitz RM, Zhang H, Vogel H, Cartwright J Jr, Dionne L, Lu N, Huang S, Matzuk MM. Neurodegeneration, myocardial injury, and perinatal death in mitochondrial superoxide dismutase-deficient mice. Proc Natl Acad Sci U S A. 1996; 93(18):9782–9787. [PubMed: 8790408]
8. Huang TT, Carlson EJ, Raineri I, Gillespie AM, Kozy H, Epstein CJ. The use of transgenic and mutant mice to study oxygen free radical metabolism. Ann N Y Acad Sci. 1999; 893:95–112. [PubMed: 10672232]
9. Van Remmen H, et al. Life-long reduction in MnSOD activity results in increased DNA damage and higher incidence of cancer but does not accelerate aging. Physiol Genomics. 2003; 16(1):29–37. [PubMed: 14679299]
10. Williams MD, Van Remmen H, Conrad CC, Huang TT, Epstein CJ, Richardson A. Increased oxidative damage is correlated to altered mitochondrial function in heterozygous manganese superoxide dismutase knockout mice. J Biol Chem. 1998; 273(43):28510–28515. [PubMed: 9774481]
11. Van Remmen H, Salvador C, Yang H, Huang TT, Epstein CJ, Richardson A. Characterization of the antioxidant status of the heterozygous manganese superoxide dismutase knockout mouse. Arch Biochem Biophys. 1999; 363(1):91–97. [PubMed: 10049502]
12. Van Remmen H, Williams MD, Guo Z, Estlack L, Yang H, Carlson EJ, Epstein CJ, Huang TT, Richardson A. Knockout mice heterozygous for Sod2 show alterations in cardiac mitochondrial

function and apoptosis. Am J Physiol Heart Circ Physiol. 2001; 281(3):H1422–H1432. [PubMed: 11514315]

13. Strassburger M, et al. Heterozygous deficiency of manganese superoxide dismutase results in severe lipid peroxidation and spontaneous apoptosis in murine myocardium in vivo. Free Radic Biol Med. 2005; 38(11):1458–1470. [PubMed: 15890620]
14. Huang TT, Yasunami M, Carlson EJ, Gillespie AM, Reaume AG, Hoffman EK, Chan PH, Scott RW, Epstein CJ. Superoxide-mediated cytotoxicity in superoxide dismutase-deficient fetal fibroblasts. Arch Biochem Biophys. 1997; 344(2):424–432. [PubMed: 9264557]
15. Tsan MF, White JE, Caska B, Epstein CJ, Lee CY. Susceptibility of heterozygous MnSOD gene-knockout mice to oxygen toxicity. Am J Respir Cell Mol Biol. 1998; 19(1):114–120. [PubMed: 9651187]
16. Kokoszka JE, Coskun P, Esposito LA, Wallace DC. Increased mitochondrial oxidative stress in the Sod2 (+/−) mouse results in the age-related decline of mitochondrial function culminating in increased apoptosis. Proc Natl Acad Sci U S A. 2001; 98(5):2278–2283. [PubMed: 11226230]
17. Asikainen TM, Huang TT, Taskinen E, Levonen AL, Carlson E, Lapatto R, Epstein CJ, Raivio KO. Increased sensitivity of homozygous Sod2 mutant mice to oxygen toxicity. Free Radic Biol Med. 2002; 32(2):175–186. [PubMed: 11796207]
18. Sarsour EH, Venkataraman S, Kalen AL, Oberley LW, Goswami PC. Manganese superoxide dismutase activity regulates transitions between quiescent and proliferative growth. Aging Cell. 2008; 7(3):405–417. [PubMed: 18331617]
19. Reiling JH, Sabatini DM. Stress and mTORture signaling. Oncogene. 2006; 25(48):6373–6383. [PubMed: 17041623]
20. Schieke SM, Finkel T. Mitochondrial signaling, TOR, and life span. Biol Chem. 2006; 387(10–11):1357–1361. [PubMed: 17081107]
21. Schieke SM, Phillips D, McCoy JP Jr, Aponte AM, Shen RF, Balaban RS, Finkel T. The mammalian target of rapamycin (mTOR) pathway regulates mitochondrial oxygen consumption and oxidative capacity. J Biol Chem. 2006; 281(37):27643–27652. [PubMed: 16847060]
22. Perez de Obanos MP, Lopez-Zabalza MJ, Arriazu E, Modol T, Prieto J, Herraiz MT, Iraburu MJ. Reactive oxygen species (ROS) mediate the effects of leucine on translation regulation and type I collagen production in hepatic stellate cells. Biochim Biophys Acta. 2007; 1773(11):1681–1688. [PubMed: 17707924]
23. Gulati P, Gaspers LD, Dann SG, Joaquin M, Nobukuni T, Natt F, Kozma SC, Thomas AP, Thomas G. Amino acids activate mTOR complex 1 via Ca2+/CaM signaling to hVps34. Cell Metab. 2008; 7(5):456–465. [PubMed: 18460336]
24. Ballou LM, Jiang YP, Du G, Frohman MA, Lin RZ. Ca(2+)- and phospholipase D-dependent and -independent pathways activate mTOR signaling. FEBS Lett. 2003; 550(1–3):51–56. [PubMed: 12935885]
25. Zhang YQ, Herman B. Expression and modification of ARC (apoptosis repressor with a CARD domain) is distinctly regulated by oxidative stress in cancer cells. J Cell Biochem. 2008
26. Zhang BX, Ma X, Zhang W, Yeh CK, Lin A, Luo J, Sprague EA, Swerdlow RH, Katz MS. Polyunsaturated fatty acids mobilize intracellular Ca2+ in NT2 human teratocarcinoma cells by causing release of Ca2+ from mitochondria. Am J Physiol Cell Physiol. 2006; 290(5):C1321–C1333. [PubMed: 16601147]
27. Muller FL, et al. Absence of CuZn superoxide dismutase leads to elevated oxidative stress and acceleration of age-dependent skeletal muscle atrophy. Free Radic Biol Med. 2006; 40(11):1993–2004. [PubMed: 16716900]
28. Roberts LJ 2nd, Oates JA, Linton MF, Fazio S, Meador BP, Gross MD, Shyr Y, Morrow JD. The relationship between dose of vitamin E and suppression of oxidative stress in humans. Free Radic Biol Med. 2007; 43(10):1388–1393. [PubMed: 17936185]
29. Zielonka J, Vasquez-Vivar J, Kalyanaraman B. Detection of 2-hydroxyethidium in cellular systems: a unique marker product of superoxide and hydroethidine. Nat Protoc. 2008; 3(1):8–21. [PubMed: 18193017]

30. Elchuri S, Oberley TD, Qi W, Eisenstein RS, Jackson Roberts L, Van Remmen H, Epstein CJ, Huang TT. CuZnSOD deficiency leads to persistent and widespread oxidative damage and hepatocarcinogenesis later in life. Oncogene. 2005; 24(3):367–380. [PubMed: 15531919]
31. Feissner RF, Skalska J, Gaum WE, Sheu SS. Crosstalk signaling between mitochondrial Ca2+ and ROS. Front Biosci. 2009; 14:1197–1218. [PubMed: 19273125]
32. Jaiswal MK, Keller BU. Cu/Zn superoxide dismutase typical for familial amyotrophic lateral sclerosis increases the vulnerability of mitochondria and perturbs Ca2+ homeostasis in SOD1G93A mice. Mol Pharmacol. 2009; 75(3):478–489. [PubMed: 19060114]
33. Zhang HM, Dang H, Yeh C, Zhang B. Linoleic acid-induced mitochondrial Ca(2+) efflux causes peroxynitrite generation and protein nitrotyrosylation.8. PLoS One. 2009; 4(6):60.
34. Zhang H, Li ZH, Zhang MQ, Katz MS, Zhang BX. Heat shock protein 90beta1 is essential for polyunsaturated fatty acid-induced mitochondrial Ca2+ efflux. J Biol Chem. 2008; 283(12):7580–7589. [PubMed: 18178560]
35. D'Autreaux B, Toledano MB. ROS as signalling molecules: mechanisms that generate specificity in ROS homeostasis. Nat Rev Mol Cell Biol. 2007; 8(10):813–824. [PubMed: 17848967]
36. Wullschleger S, Loewith R, Hall MN. TOR signaling in growth and metabolism. Cell. 2006; 124(3):471–484. [PubMed: 16469695]
37. Klionsky DJ, et al. Guidelines for the use and interpretation of assays for monitoring autophagy in higher eukaryotes. Autophagy. 2008; 4(2):151–175. [PubMed: 18188003]
38. Morten KJ, Ackrell BA, Melov S. Mitochondrial reactive oxygen species in mice lacking superoxide dismutase 2: attenuation via antioxidant treatment. J Biol Chem. 2006; 281(6):3354–3359. [PubMed: 16326710]
39. Melov S, Doctrow SR, Schneider JA, Haberson J, Patel M, Coskun PE, Huffman K, Wallace DC, Malfroy B. Lifespan extension and rescue of spongiform encephalopathy in superoxide dismutase 2 nullizygous mice treated with superoxide dismutase-catalase mimetics. J Neurosci. 2001; 21(21):8348–8353. [PubMed: 11606622]
40. Cuzzocrea S, Costantino G, Mazzon E, Zingarelli B, De Sarro A, Caputi AP. Protective effects of Mn(III)tetrakis (4-benzoic acid) porphyrin (MnTBAP), a superoxide dismutase mimetic, in paw oedema induced by carrageenan in the rat. Biochem Pharmacol. 1999; 58(1):171–176. [PubMed: 10403531]
41. Sharma SS, Gupta S. Neuroprotective effect of MnTMPyP, a superoxide dismutase/catalase mimetic in global cerebral ischemia is mediated through reduction of oxidative stress and DNA fragmentation. Eur J Pharmacol. 2007; 561(1–3):72–79. [PubMed: 17320858]
42. Van Remmen H, et al. Multiple deficiencies in antioxidant enzymes in mice result in a compound increase in sensitivity to oxidative stress. Free Radic Biol Med. 2004; 36(12):1625–1634. [PubMed: 15182862]
43. Blagosklonny MV. Aging: ROS or TOR. Cell Cycle. 2008; 7(21):3344–3354. [PubMed: 18971624]
44. Perez VI, Van Remmen H, Bokov A, Epstein CJ, Vijg J, Richardson A. The Overexpression of Major Antioxidant Enzymes Does Not Extend the Lifespan of Mice. Aging Cell. 2008
45. Muller FL, Lustgarten MS, Jang Y, Richardson A, Van Remmen H. Trends in oxidative aging theories. Free Radic Biol Med. 2007; 43(4):477–503. [PubMed: 17640558]
46. Jang YC, Remmen VH. The mitochondrial theory of aging: insight from transgenic and knockout mouse models. Exp Gerontol. 2009; 44(4):256–260. [PubMed: 19171187]
47. Chevallet M, Wagner E, Luche S, van Dorsselaer A, Leize-Wagner E, Rabilloud T. Regeneration of peroxiredoxins during recovery after oxidative stress: only some overoxidized peroxiredoxins can be reduced during recovery after oxidative stress. J Biol Chem. 2003; 278(39):37146–37153. [PubMed: 12853451]
48. Chiribau CB, Cheng L, Cucoranu IC, Yu YS, Clempus RE, Sorescu D. FOXO3A regulates peroxiredoxin III expression in human cardiac fibroblasts. J Biol Chem. 2008; 283(13):8211–8217. [PubMed: 18195003]
49. Takada S, et al. Generation and characterization of cells that can be conditionally depleted of mitochondrial SOD2. Biochem Biophys Res Commun. 2009; 379(2):233–238. [PubMed: 19100713]

50. Kim A, Joseph S, Khan A, Epstein CJ, Sobel R, Huang TT. Enhanced expression of mitochondrial superoxide dismutase leads to prolonged in vivo cell cycle progression and up-regulation of mitochondrial thioredoxin. Free Radic Biol Med.
51. Kalen AL, Sarsour EH, Venkataraman S, Goswami PC. Mn-superoxide dismutase overexpression enhances G2 accumulation and radioresistance in human oral squamous carcinoma cells. Antioxid Redox Signal. 2006; 8(7–8):1273–1281. [PubMed: 16910775]
52. Kannoji A, Phukan S, Sudher Babu V, Balaji VN. GSK3beta: a master switch and a promising target. Expert Opin Ther Targets. 2008; 12(11):1443–1455. [PubMed: 18851699]
53. Moore MN. Autophagy as a second level protective process in conferring resistance to environmentally-induced oxidative stress. Autophagy. 2008; 4(2):254–256. [PubMed: 18196967]
54. Vellai T, Bicsak B, Toth ML, Takacs-Vellai K, Kovacs AL. Regulation of cell growth by autophagy. Autophagy. 2008; 4(4):507–509. [PubMed: 18259117]
55. Scherz-Shouval R, Elazar Z. ROS, mitochondria and the regulation of autophagy. Trends Cell Biol. 2007; 17(9):422–427. [PubMed: 17804237]
56. Hidalgo C, Donoso P. Crosstalk between calcium and redox signaling: from molecular mechanisms to health implications. Antioxid Redox Signal. 2008; 10(7):1275–1312. [PubMed: 18377233]
57. Whitaker M. Calcium signalling in early embryos. Philos Trans R Soc Lond B Biol Sci. 2008; 363(1495):1401–1418. [PubMed: 18263556]
58. Camello-Almaraz C, Gomez-Pinilla PJ, Pozo MJ, Camello PJ. Mitochondrial reactive oxygen species and Ca2+ signaling. Am J Physiol Cell Physiol. 2006; 291(5):C1082–C1088. [PubMed: 16760264]
59. Gordeeva AV, Zvyagilskaya RA, Labas YA. Cross-talk between reactive oxygen species and calcium in living cells. Biochemistry (Mosc). 2003; 68(10):1077–1080. [PubMed: 14616077]
60. Genestra M. Oxyl radicals, redox-sensitive signalling cascades and antioxidants. Cell Signal. 2007; 19(9):1807–1819. [PubMed: 17570640]
61. Afanas'ev IB. Signaling functions of free radicals superoxide & nitric oxide under physiological & pathological conditions. Mol Biotechnol. 2007; 37(1):2–4. [PubMed: 17914156]
62. Finkel T. Reactive oxygen species and signal transduction. IUBMB Life. 2001; 52(1–2):3–6. [PubMed: 11795590]
63. Wu AL, Kim JH, Zhang C, Unterman TG, Chen J. Forkhead box protein O1 negatively regulates skeletal myocyte differentiation through degradation of mammalian target of rapamycin pathway components. Endocrinology. 2008; 149(3):1407–1414. [PubMed: 18079193]
64. Kamata H, Honda S, Maeda S, Chang L, Hirata H, Karin M. Reactive oxygen species promote TNFalpha-induced death and sustained JNK activation by inhibiting MAP kinase phosphatases. Cell. 2005; 120(5):649–661. [PubMed: 15766528]
65. Pelaia G, et al. Effects of hydrogen peroxide on MAPK activation, IL-8 production and cell viability in primary cultures of human bronchial epithelial cells. J Cell Biochem. 2004; 93(1):142–152. [PubMed: 15352171]

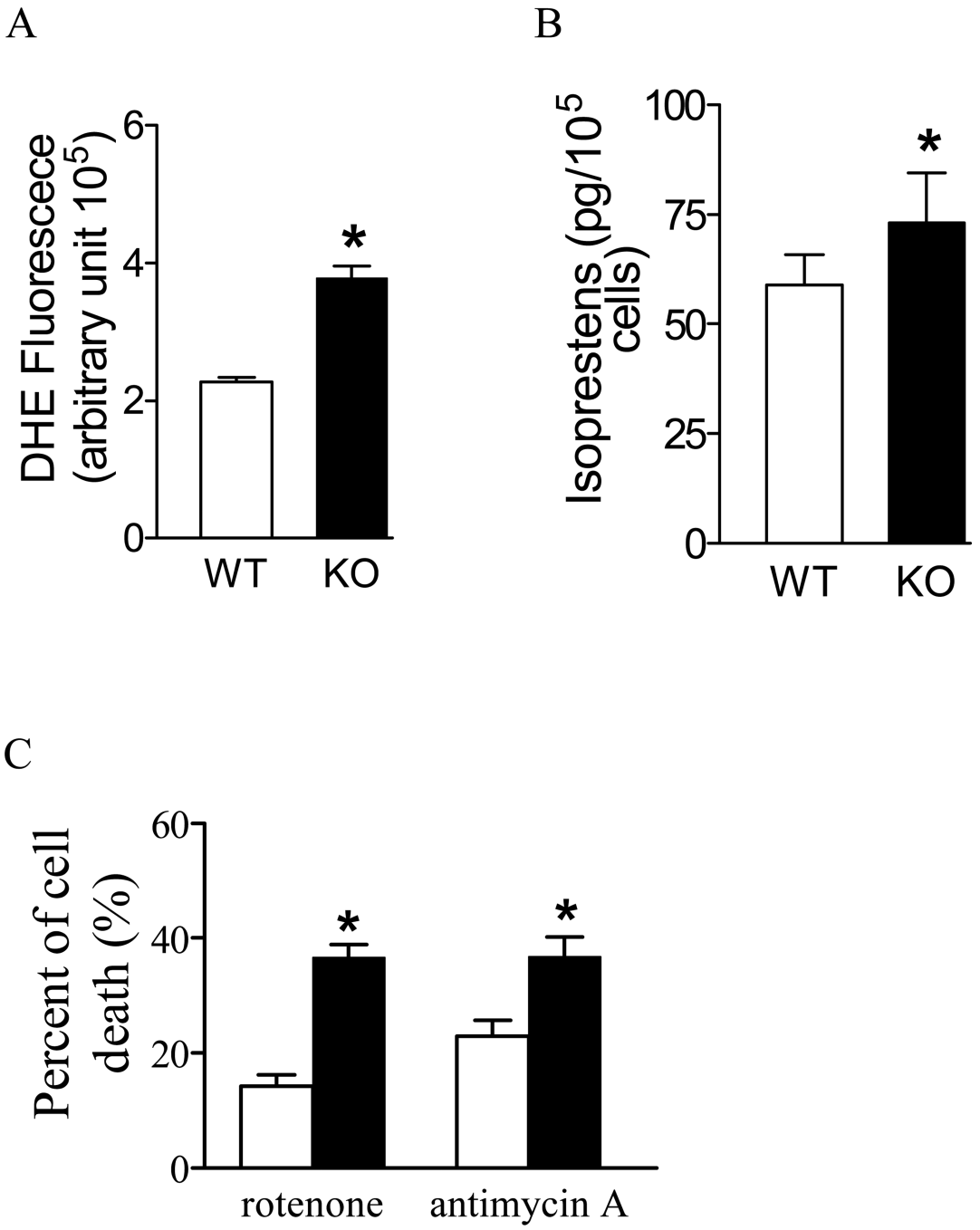

Figure 1. Sensitivity of *Sod2*$^{-/-}$ cells to oxidative stress and endogenous ROS generation

(A) ROS measurement with DHE using whole cell as described in the Materials and Methods section; (B) Lipid oxidation measured as the isoprostane contents. (C) Sensitivity of *Sod2*$^{-/-}$ cells to inhibitors of mitochondrial respiratory chain. Cell viability was measured using the MTT assay as described in the Materials and Methods section. *$p < 0.05$ and ** $p < 0.01$ between wild-type (WT) and *Sod2*$^{-/-}$ (KO) groups (n=3 experiments).

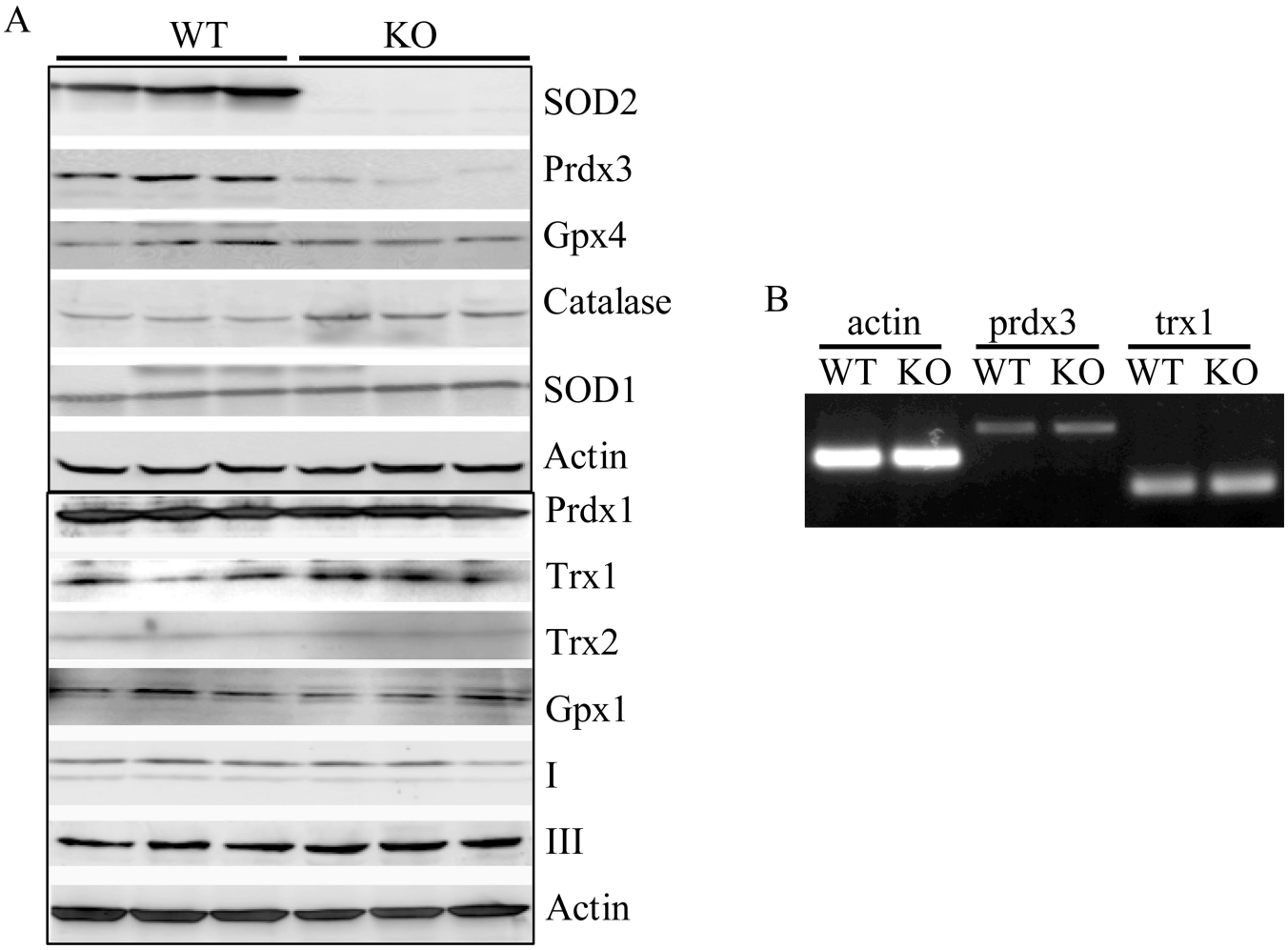

Figure 2. Expression of anti-oxidative stress enzymes in *Sod2*$^{-/-}$ MEFs

(A) Western blot analysis of whole cell lysate from three individual wild-type (WT) and *Sod2*$^{-/-}$ MEFs (KO) was performed as described in the Materials and Methods section. Protein band intensity was quantified as described in the Materials and Methods section. (B) Semi-Quantitative RT-PCR analysis of mRNA level of *prdx3* and *trx1*.

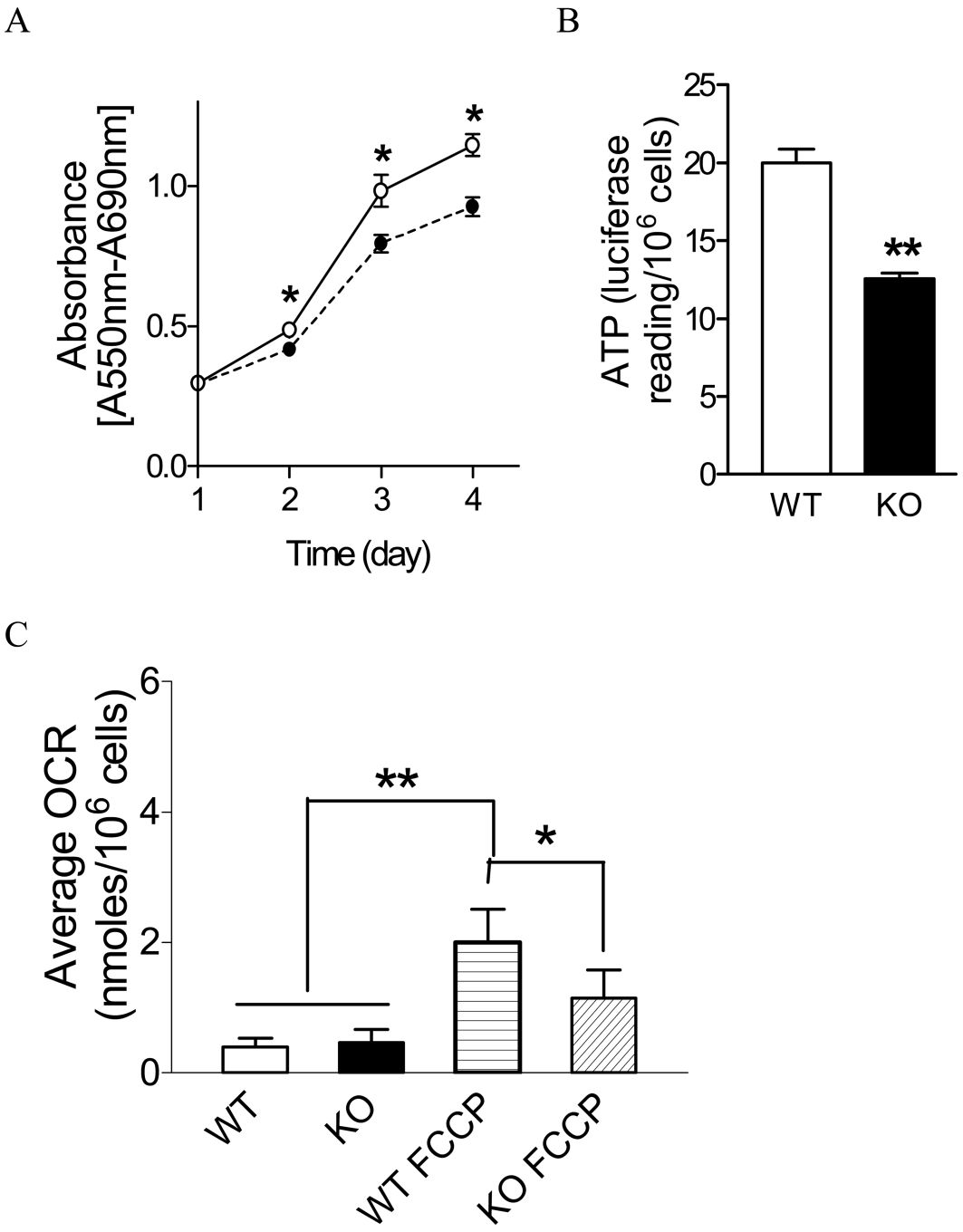

Figure 3. Proliferation of *Sod2*$^{-/-}$ cells and mitochondrial function

(A) Wild-type (solid line with open circle (○)) and *Sod2*$^{-/-}$ cells (dotted line with solid circle (●)) were seeded equally onto 96-well plates as described in the Materials and Methods section. Cell growth was monitored by MTT assay every 24 hours. Data represent three different experiments. *$p < 0.05$ between wild-type and *Sod2*$^{-/-}$ MEFs at each time point. (B) ATP production measured in whole cell. **$p < 0.01$ between wild-type and *Sod2*$^{-/-}$ MEFs. (C) Oxygen consumption (OCR) measured by Seahorse Bioscience Extracellular Flux Analyzer XF24. *$p < 0.05$ between wild-type and *Sod2*$^{-/-}$ MEFs treated with FCCP; **$p < 0.05$ between untreated and FCCP-treated cells. WT: wild type; KO: *Sod2*$^{-/-}$ MEF.

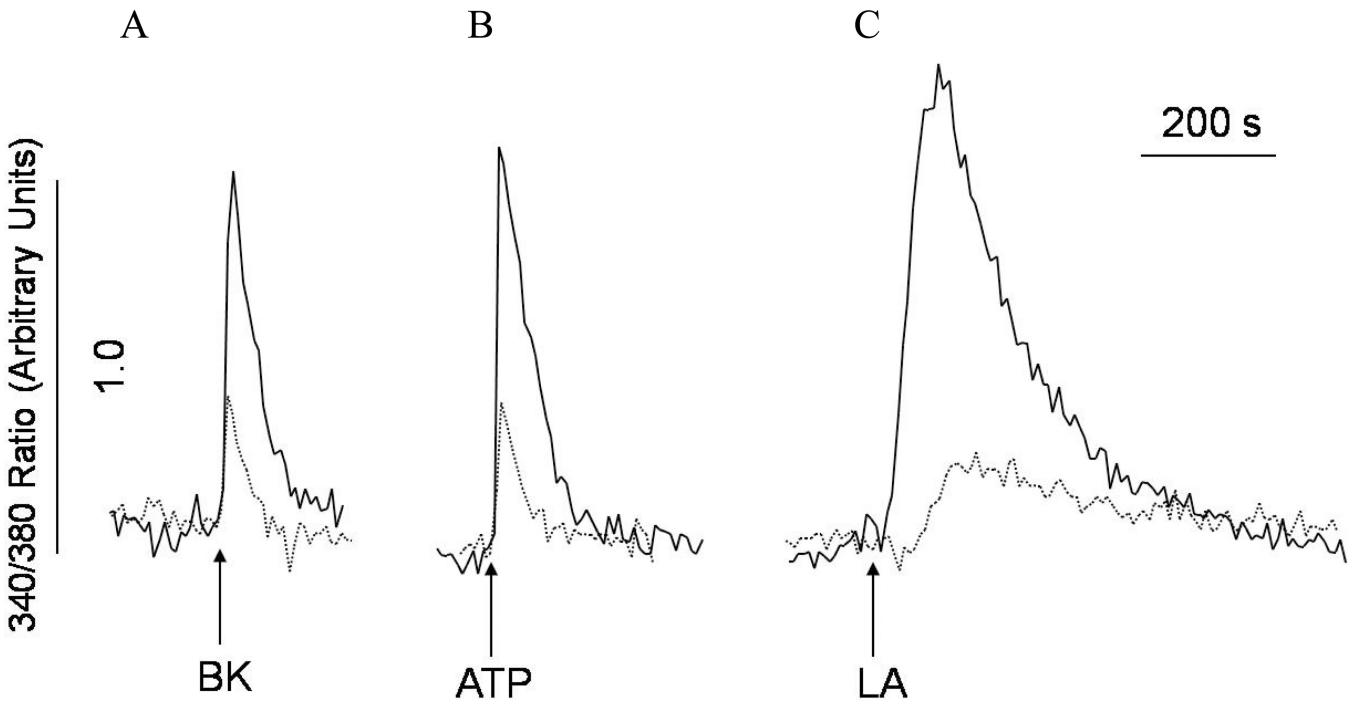

Figure 4. Abnormal intracellular Ca^{2+} signaling in *Sod2*$^{-/-}$ MEF

Both wild-type (WT) and *Sod2*$^{-/-}$ MEFs (KO) were labeled with fura-2 AM (1 μM, 30 minutes) to monitor changes of intracellular Ca^{2+}. Wild-type (solid traces) or *Sod2*$^{-/-}$ MEF (dashed traces) in suspension were either stimulated with (A) bradykinin (100 nM), (B) ATP (100 μM), or (C) linoleic acid (30 μM) as indicated by arrows in the figure. The traces are representative of three experiments.

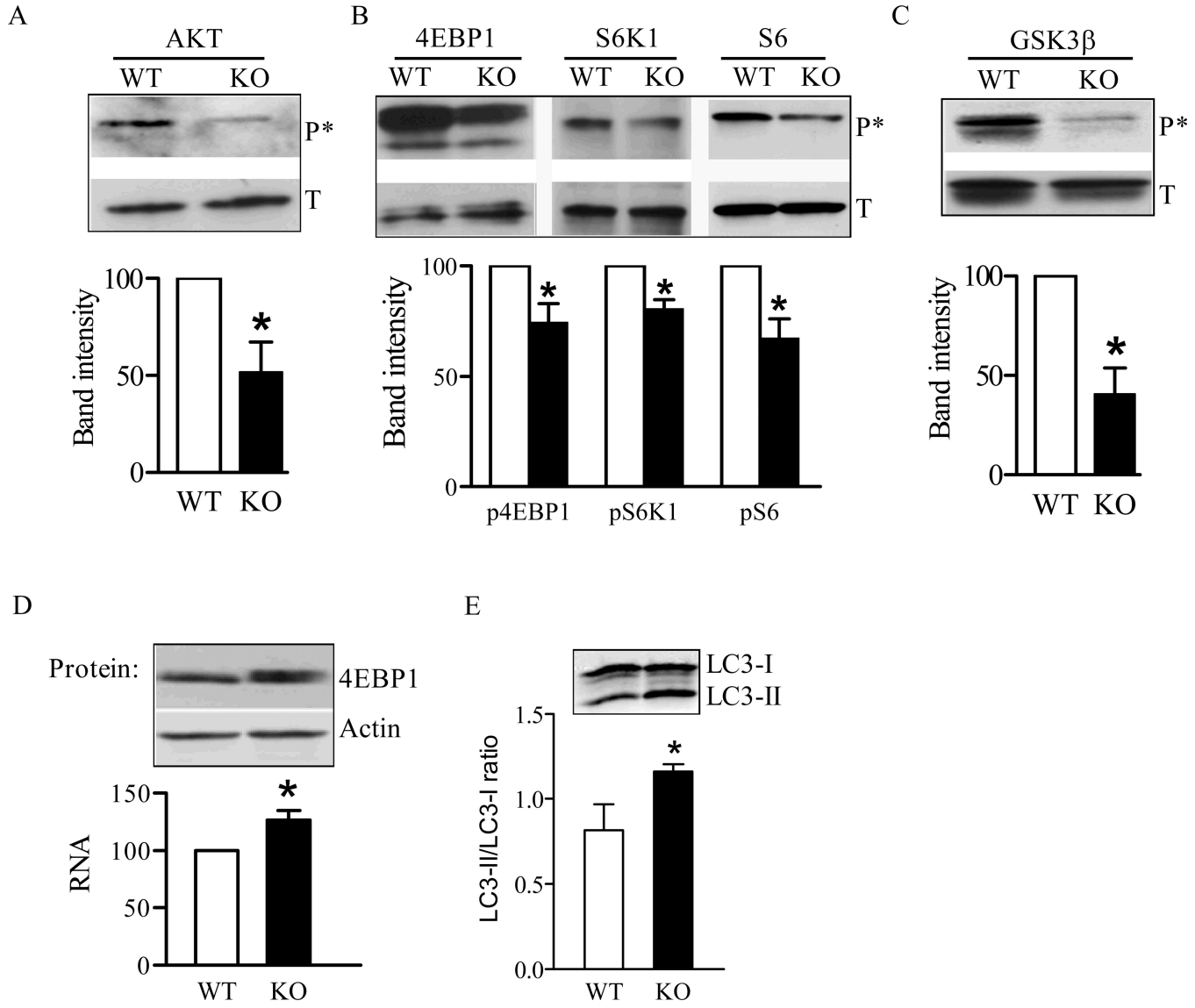

Figure 5. Abnormal cell signaling in *Sod2*$^{-/-}$ MEFs

Phosphorylation of different signaling proteins were detected with phosphorylation specific antibodies as described in the Materials and Methods section: (A) Phosphorylation of Akt; (B) Phosphorylation of 4EBP1, p76SK1, and S6; (C) Phosphorylation of GSK3. (D) Expression of 4EBP1 in *Sod2*$^{-/-}$ cells detected as mRNA transcription by real-time quantitative RT-PCR (lower graph) and as protein by Western blot analysis (upper panel). (E) Detection of autophagy by Western blot analysis of LC3 modification. Differences of band intensity between wild-type (WT) and *Sod2*$^{-/-}$ MEFs (KO) were presented in the lower graph. *$p < 0.05$ and **$p < 0.01$ between WT and *Sod2*$^{-/-}$ cells for respective target protein. Data were generated from three different experiments.

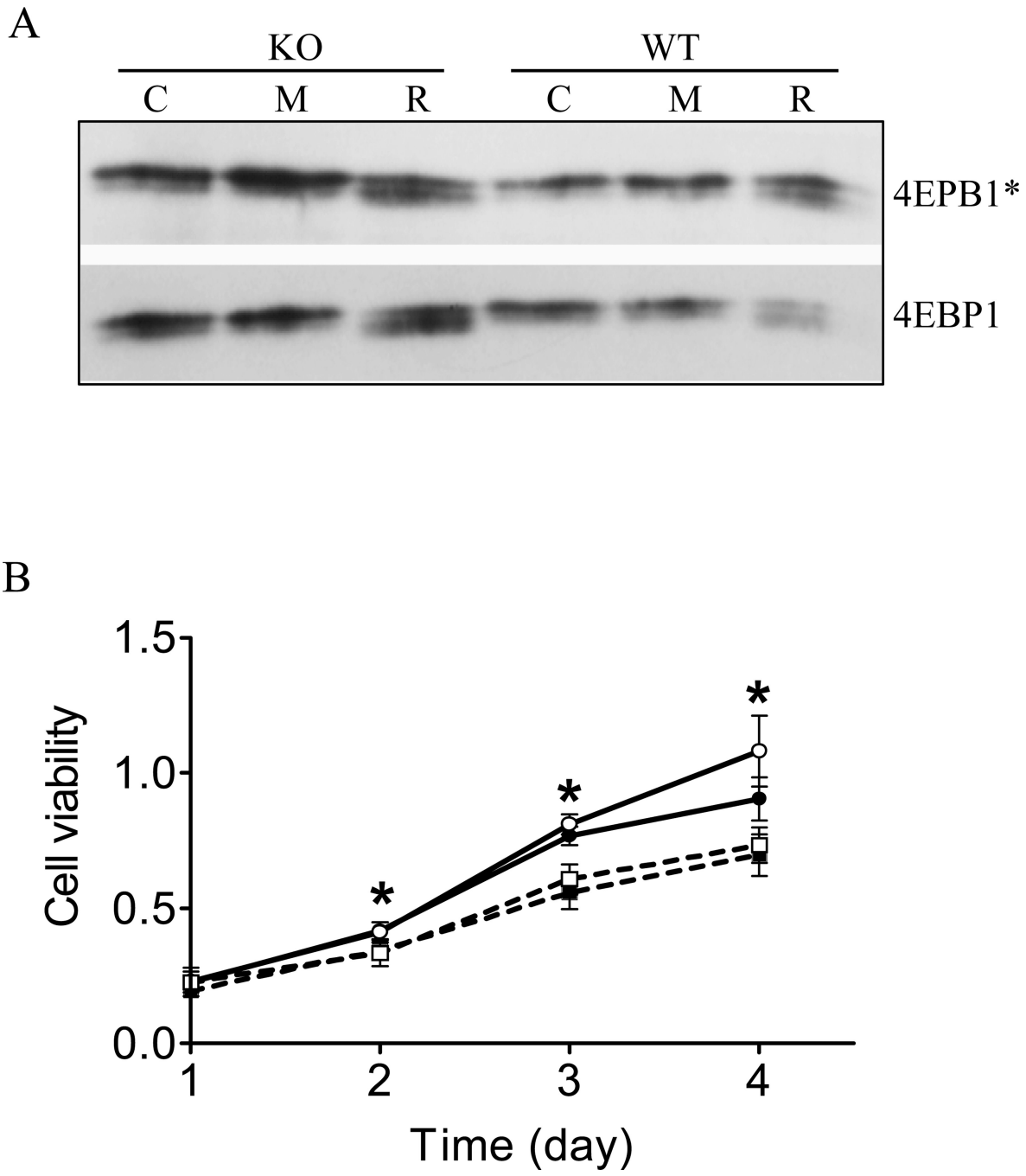

Figure 6. The SOD mimetic, MnTBAP failed to rescue the slow growth of *Sod2*$^{-/-}$ MEFs

(A) MnTBAP partially restored phosphorylation of 4EBP1 in *Sod2*$^{-/-}$ MEFs. MEFs were treated with medium (C, open bar), 200 nM rapamycin (R, solid bar) or 400 μM MnTBAP for 4 hours before harvested for protein analysis. *4EBP1 indicates phosphorylated protein. (B) Proliferation of MEFs in response to MnTBAP. MEFs were incubated with 0, or 400 μM MnTBAP for 4 days. Open circle (○): wild-type MEF; solid circle (●): wild-type MEF with MnTBAP; open square (□): *Sod2*$^{-/-}$ MEF; solid square (■): *Sod2*$^{-/-}$ MEF with MnTBAP. *$p < 0.05$ between wild-type and *Sod2*$^{-/-}$ MEFs at each time point.

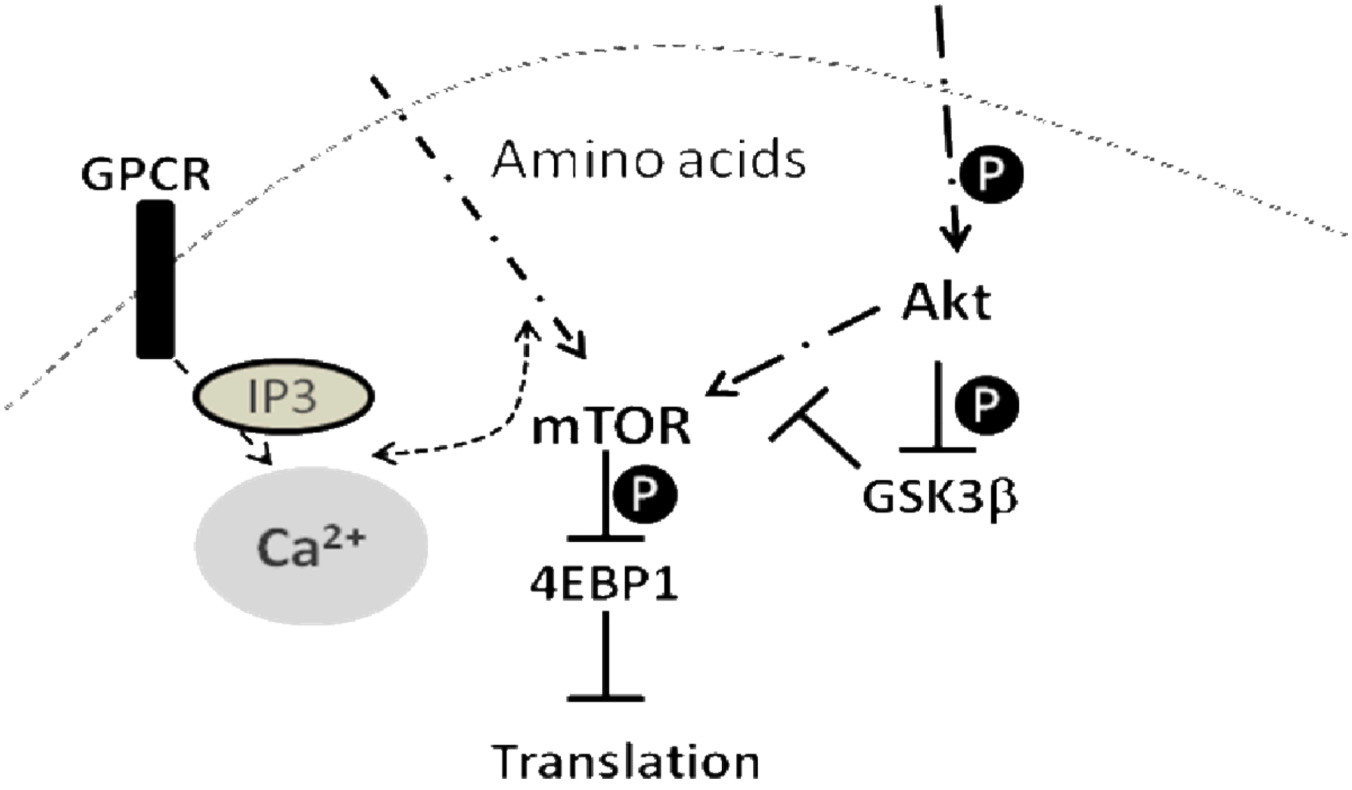

Figure 7.
A simplified diagram of how mTOR, GSK3β, Ca^{2+} homeostasis interact with each other to affect cell growth. GPCR - G-protein coupled receptor; IP3 – inositol trisphosphate.